Saudi Journal of Biological Sciences 29 (2022) 103297

Contents lists available at ScienceDirect

Saudi Journal of Biological Sciences

journal homepage: www.sciencedirect.com

Original article

An *in silico* approach unveils the potential of antiviral compounds in preclinical and clinical trials as SARS-CoV-2 omicron inhibitors

Arun Bahadur Gurung [a,*], Mohammad Ajmal Ali [b], Mohamed S. Elshikh [b], Ibrahim Aref [b], Musarat Amina [c], Joongku Lee [d]

[a] Department of Basic Sciences and Social Sciences, North-Eastern Hill University, Shillong 793022, Meghalaya, India
[b] Department of Botany and Microbiology, College of Science, King Saud University, P.O. Box 2455, Riyadh 11451, Saudi Arabia
[c] Department of Pharmacognosy, Pharmacy College, King Saud University, Riyadh 11451, Saudi Arabia
[d] Department of Environment and Forest Resources, Chungnam National University, 99 Daehak-ro, Yuseong-gu, Daejeon 34134, Republic of Korea

ARTICLE INFO

Article history:
Received 26 January 2022
Revised 12 March 2022
Accepted 17 April 2022
Available online 22 April 2022

Keywords:
Omicron
Variant of concern
SARS-CoV-2 omicron
COVID-19
Abemaciclib
Dasatinib
Spiperone
Molecular docking
Molecular dynamics simulations

ABSTRACT

The increased transmissibility and highly infectious nature of the new variant of concern (VOC) that is severe acute respiratory syndrome coronavirus 2 (SARS-CoV-2) Omicron and lack of effective therapy need the rapid discovery of therapeutic antivirals against it. The present investigation aimed to identify antiviral compounds that would be effective against SARS-CoV-2 Omicron. In this study, molecular docking experiments were carried out using the recently reported experimental structure of omicron spike protein in complex with human angiotensin-converting enzyme 2 (ACE2) and various antivirals in preclinical and clinical trial studies. Out of 36 tested compounds, Abemaciclib, Dasatinib and Spiperone are the three top-ranked molecules which scored binding energies of −10.08 kcal/mol, −10.06 kcal/mol and −9.54 kcal/mol respectively. Phe338, Asp339, and Asp364 are crucial omicron receptor residues involved in hydrogen bond interactions, while other residues were mostly involved in hydrophobic interactions with the lead molecules. The identified lead compounds also scored well in terms of drug-likeness. Molecular dynamics (MD) simulation, essential dynamics (ED) and entropic analysis indicate the ability of these molecules to modulate the activity of omicron spike protein. Therefore, Abemaciclib, Dasatinib and Spiperone are likely to be viable drug-candidate molecules that can block the interaction between the omicron spike protein and the host cellular receptor ACE2. Though our findings are compelling, more research into these molecules is needed before they can be employed as drugs to treat SARS-CoV-2 omicron infections.

1. Introduction

The increased daily reported cases of coronavirus disease 2019 (COVID-19) due to the Omicron variant (B.1.1.529) of severe acute respiratory syndrome coronavirus 2 (SARS-CoV-2) has added further to the global health crisis. This new variant of concern (VOC) was first detected on November, 1 in Botswana and reported to the World Health Organization (WHO) on November 26, 2021. Since then, it has rapidly spread to at least 38 countries (WHO Classification of Omicron (B.1.1.529), 2021). Omicron features a few deletions and over 30 mutations, some of which (e.g., 69–70del, T95I, G142D/143–145del, K417N, T478K, N501Y, N655Y, N679K, and P681H) overlap with those seen in the alpha, beta, gamma, or delta VOC (GISAID, 2021). These deletions and mutations have been linked to its increased transmissibility, stronger viral binding affinity, and antibody escape. Other known omicron mutations include those that improve transmissibility and alter binding affinity (Greaney et al., 2021; Harvey et al., 2021). Unfortunately, the implications of the majority of the remaining omicron mutations are unknown, leaving a lot of questions about how the whole set of deletions and mutations may affect viral behaviour and vulnerability to natural and vaccine-mediated immunity (Karim and Karim, 2021). This fifth VOC is considered to be three times more contagious than the original SARS-CoV-2 and maybe even more so than the delta variant (Gao et al., 2021).

* Corresponding author.
E-mail address: arunbgurung@gmail.com (A. Bahadur Gurung).
Peer review under responsibility of King Saud University.

Production and hosting by Elsevier

https://doi.org/10.1016/j.sjbs.2022.103297
1319-562X/

Computational drug discovery is a successful technique for speeding up and reducing the cost of drug development. The applicability of computational drug discovery has been extended and broadly applied to nearly every stage in the drug discovery and development workflow, including target identification and validation, lead discovery and optimization, and preclinical tests, due to the dramatic increase in the availability of biological macromolecule and small molecule information (Ou-Yang et al., 2012). One of the most extensively utilised structure-based drug design (SBDD) methods is virtual screening based on molecular docking. The molecular docking approach may be used to represent the atomic level interaction between a small molecule and a protein, allowing us to define small molecule behaviour in target protein binding sites and elucidate essential biochemical processes (McConkey et al., 2002). The technique is becoming increasingly popular in computer-aided drug design as more biomolecular structures are being submitted to the protein data bank and made freely available. However, standard molecular docking approaches do not take into account the target's flexibility, which could lead to the omission of some active molecules. Molecular dynamics (MD) simulations, on the other hand, may obtain numerous target conformations and have been frequently employed in molecular docking to account for target flexibility (Liu et al., 2018). MD simulations paired with binding free energy estimates have also been found to be an effective technique for increasing the enrichment factor of virtual screening by improving the accuracy of target-ligand binding ability prediction (Rastelli et al., 2010). The recently solved experimental structure of SARS-CoV-2 Omicron spike protein in complex with human ACE2 (PDB ID: 7WBL) (Han et al., 2022) offers an opportunity to identify small molecule inhibitors. The transmembrane spike (S) glycoprotein, which forms homotrimers projecting from the viral surface, is responsible for coronavirus (CoV) entry into host cells (Tortorici and Veesler, 2019). S is made up of two functional subunits that are responsible for viral and cellular membrane fusion (S1 subunit) as well as binding to the host cell receptor (S2 subunit). S is cleaved at the interface between the S1 and S2 subunits in many CoVs, although they remain non-covalently coupled in the prefusion conformation (Kirchdoerfer et al., 2016; Walls et al., 2016). S is cleaved further by host proteases at the so-called S2′ site, which is positioned immediately upstream of the fusion peptide in all CoVs (Madu et al., 2009; Millet and Whittaker, 2015). It's been suggested that this cleavage prepares the protein for membrane fusion by causing substantial irreversible conformational changes (Park et al., 2016). The coronavirus S glycoprotein is the principal target of neutralising antibodies (Abs) and the focus of therapeutic and vaccine design because it is surface-exposed and mediates viral entry into host cells (Walls et al., 2020). In this study, we have used the molecular docking technique and molecular dynamics simulations to screen small antiviral molecules which can effectively bind to the omicron spike protein and hinder its interaction with the host cellular receptor. We have proposed a few molecules which may be developed into antiviral drugs against omicron.

2. Materials and methods

2.1. Retrieval of ligands and protein structure

A total of 36 compounds with preclinical or clinical trial evidence against previous variants of SARS-CoV-2 were selected for the study (Xiang et al., 2021). The three-dimensional structures of the compounds were obtained from the PubChem database (Kim et al., 2016). The compounds with the 2D structure were converted into the 3D structure using OpenBabel version 2.4.1 (O'Boyle et al., 2011). The structural optimization of the compounds was performed using the Merck molecular force field 94 (MMFF94) (Halgren, 1996). The three-dimensional structure of SARS-CoV-2 Omicron spike protein in complex with human ACE2 was retrieved from protein data bank (PDB) using accession PDB ID: 7WBL (Han et al., 2022). The cryogenic electron microscopy (cryo-EM) structure has been resolved at a resolution of 3.40 Å.

2.2. Evaluation of interface statistics of a complex between omicron spike protein and human ACE2

The protein–protein interface statistics such as interface residues, interface area, hydrogen bonds, disulphide bonds and non-bonded contacts were evaluated using the PDBsum program (Laskowski, 2009).

2.3. Preparation of ligands and protein

Each compound was prepared for molecular docking experiments by the addition of Gasteiger charges, hydrogen atoms and optimally defined torsions using AutoDock Tools-1.5.6 (Morris et al., 2009). The heteroatoms, including ions, co-crystallized ligand and water molecules, were removed from the Omicron spike protein. AutoDock Tools-1.5.6 tool (Morris et al., 2009) was used for adding a suitable number of polar hydrogen atoms and Kollman charges to the target protein.

2.4. Molecular docking

The Lamarckian genetic algorithm was employed for molecular docking experiments where the docking parameters were selected from our previously reported methodology (Gurung, 2020). AutoDock4.2 software was used to perform blind molecular docking (Morris et al., 2009) The binding site of the compounds was defined by choosing a grid box centred at the omicron spike protein with XYZ coordinates of 79.4618, 96.1430 and 124.0359, number of grid points of 96 × 141 × 154 and grid spacing of 0.375 Å. For each compound, a total of fifty separate docking runs were performed. The docking poses were conformationally clustered using a root mean square deviation (RMSD) cut-off value of 2.0 Å. The most favourable binding poses of the compounds were explored by determining the lowest binding free energy (ΔG). The hydrogen bonds and hydrophobic interactions between the compounds and the target protein were investigated using the LigPlot^{+} v.1.4.5 tool (Laskowski and Swindells, 2011).

2.5. Evaluation of physicochemical properties of compounds

The DataWarrior version 4.6.1 program was used to determine the physicochemical characteristics of the compounds (Sander et al., 2015).

2.6. Molecular dynamics simulations

GROningen MAchine for Chemical Simulations (GROMACS) 2019.2 software (Hess et al., 2008) with the GROMOS96 43a1 force field was used to run 100-ns MD simulations on the free omicron spike protein and its complexes with lead molecules. Using a three-point model for water termed simple point charge (SPC216), the systems were solvated in a water-filled 3-D cube with 1 Å spacing. A leap-frog temporal integration technique was used to integrate Newton's equations of motion. The systems were neutralised, and the quantity of energy used was optimised. The temperature was set to 300 K, and the systems were equilibrated for 300 ps in the NVT (Number of particles, Volume, and Temperature) ensemble, and another 300 ps in the NPT (Number of particles, Pressure, and Temperature) ensemble.

2.7. Essential dynamics

Essential dynamics (ED), also known as principal component analysis (PCA), was investigated by diagonalizing a covariance matrix of C-α atoms of the system. Eigenvectors were used to define the directions of massive coordinated motions, and the eigenvalues corresponded to mean-square positional fluctuation (Amadei et al., 1993).

3. Results

A total of 36 small molecule inhibitors with preclinical and clinical trial data against COVID-19 were selected for the present study (Table 1). The rationale behind the selection of these molecules is to see if they work against the omicron variant of SARS-CoV-2 as well. We have utilised the very recently reported experimental structure of omicron SARS-CoV-2 spike with human ACE2 receptor for our studies. PDBsum analysis reveals that the protein–protein complex is stabilized through one salt bridge, ten hydrogen bonds and 87 non-bonded contacts (Table 2). The interaction of omicron spike protein to ACE2 involves Ser19, Gln24, Thr27, Phe28, Lys31, His34, Glu35, Asp38, Tyr41, Gln42 Leu79, Met82, Tyr83, Lys353, Gly354, Asp355 and Arg357 of ACE2 and Tyr449, Arg493, Tyr453, Leu455, Phe456, Ala475, Gly476, Asn477, Phe486, Asn487, Tyr489, Ser496, Arg498, Thr500, Tyr501, Gly502 and His505 of omicron spike protein (Fig. 1). The top 3 lead molecules which show considerable binding affinity to the omicron spike protein receptor include Abemaciclib (ΔG = −10.08 kcal/mol), Dasatinib (ΔG = −10.06 kcal/mol) and Spiperone (ΔG = −9.54 kcal/mol) (Table 1). These molecules bind to the spike interface region hydrophobic interactions and hydrogen bonds. For example, Abemaciclib binds to the spike protein through hydrophobic interactions with Tyr365, Leu368, Tyr369, Asn370, Phe374, Phe377, Cys379, Val382, Ser383, Pro384, Leu387, Asn388, Cys432, Ile434 and Phe515 (Fig. 2**A**). The second lead Dasatinib binds to spike protein with four hydrogen bonds-a 2.79 Å length hydrogen bond with O atom of Asp364, 2.90 Å and 2.76 Å length hydrogen bonds with OD1 atom of Asp339 and a 3.05 Å hydrogen bond with O atom of Arg457 and hydrophobic interactions with Phe342, Tyr365, Leu368, Pro373, Phe374, Phe377, Cys432, Ile434, Trp436 and Leu513 (Fig. 2**B**). The third lead molecule Spiperone binds to the spike protein receptor through hydrophobic interactions with Phe318, Asp339, Asp364, Tyr365, Val367, Leu368, Tyr369, Phe377, Pro384, Cys432, Ile434 and Leu513 (Fig. 2**C**). The compounds were also evaluated for their oral bioavailability which includes parameters such as molecular weight (MW), LogP (partition coefficient between *n*-octanol and water), number of hydrogen bond donors (HBD), number of hydrogen bond acceptors (HBA), rotatable bond (RB) count, topological polar surface area (TPSA) and drug-likeness scores (Table 3). All the three identified lead molecules-Abemaciclib, Dasatinib and Spiperone show good drug-likeness scores of 6.2983, 8.0376 and 9.9352 respectively. Although Abemaciclib's molecular weight exceeds 500, its other physicochemical properties are within the permissible range of Lipinski's rule of five (Lipinski, 2004) and Veber's rule (Veber et al., 2002), and the other two lead compounds, Dasatinib and Spiperone, totally obey these two drug-likeness rules.

The conformational changes and stability of the free omicron spike protein and its complexes with the top three lead compounds (Abemaciclib, Dasatinib, and Spiperone) were investigated using a

Table 1
Binding energy of selected compounds docked with Omicron spike protein.

S No.	compounds	Known molecular targets	PubChem CID	Binding Energy (kcal/mol)
1	Salvianolic acid C	Entry inhibitors	13991590	−5.82
2	Arbidol	Entry inhibitors	131411	−4.99
3	Cepharanthine	Entry inhibitors	10206	−7
4	Abemaciclib	Entry inhibitors	46220502	−5.74
5	Osimertinib	Entry inhibitors	71496458	−5.47
6	Trimipramine	Entry inhibitors	5584	−5.8
7	Colforsin	Entry inhibitors	47936	−6.38
8	Ingenol	Entry inhibitors	442042	−6.07
9	Clofazimine	Entry inhibitors	2794	−6.33
10	Tafenoquine	$3CL^{pro}$ inhibitors	115358	−4.77
11	Baicalin	$3CL^{pro}$ inhibitors	64982	−5.71
12	Baicalein	$3CL^{pro}$ inhibitors	5281605	−7.45
13	Cinanserin	$3CL^{pro}$ inhibitors	5475158	−5.3
14	GC373	$3CL^{pro}$ inhibitors	78225172	−5.07
15	Boceprevir	$3CL^{pro}$ inhibitors	10324367	−5.01
16	Bepridil	$3CL^{pro}$ inhibitors	2351	−4.67
17	Nelfinavir mesylate	$3CL^{pro}$ inhibitors	64142	−5.32
18	Z-FA-FMK	$3CL^{pro}$ inhibitors	5311161	−5.07
19	Suramin	$3CL^{pro}$ inhibitors	5361	−9.51
20	Lopinavir	$3CL^{pro}$ inhibitors	92727	−4.86
21	Ritonavir	$3CL^{pro}$ inhibitors	392622	−3.57
22	Dipyridamole	$3CL^{pro}$ inhibitors	3108	−2.05
23	Dasatinib	PL^{pro} inhibitors	3062316	−6.45
24	Dronedarone	PL^{pro} inhibitors	208898	−5.23
25	Remdesivir	RdRp inhibitors	121304016	−3.17
26	Favipiravir	RdRp inhibitors	492405	−4.56
27	Dolutegravir	RdRp inhibitors	54726191	−7.21
28	β-D-N4-Hydroxycytidine (EIDD-1931)	RdRp inhibitors	197020	−5.39
29	Tipranavir	Other small molecule inhibitors	54682461	−5.42
30	Saquinavir	Other small molecule inhibitors	441243	−5.93
31	Atazanavir	Other small molecule inhibitors	148192	−4.31
32	Azithromycin	Other small molecule inhibitors	447043	−3.2
33	Spiperone	Other small molecule inhibitors	5265	−6.76
34	Alprostadil	Other small molecule inhibitors	5280723	−6.23
35	Ivermectin	Other small molecule inhibitors	6321424	−6.95
36	Penciclovir	Other small molecule inhibitors	135398748	−5.17

Table 2
Interface statistics of ACE2:Omicron spike protein complex.

Complex	Chain	No. of interface residues	Interface Area (Å^2)	No. of salt bridges	No. of disulphide bonds	No. of hydrogen bonds	No. of non-bonded contacts
ACE2:Omicron Spike protein complex	A (ACE2)	17	829	1	–	10	87
	B (Omicron spike protein)	17	877				

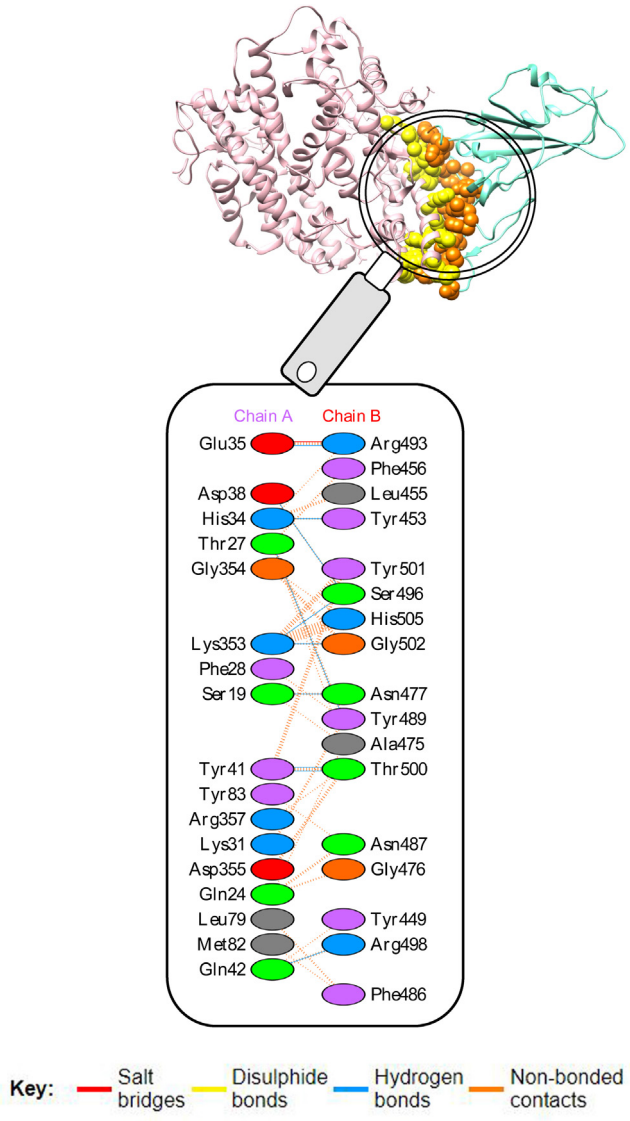

Fig. 1. **(A)** Protein-protein complex between human ACE2 (pink) and omicron spike protein (aquamarine) and with the interface residues shown in yellow and orange spheres for ACE2 and spike protein respectively. **(B)** PDBSum analysis shows the interface residues and molecular interactions between ACE2 (Chain A) and omicron spike (Chain B).

100-ns molecular dynamics simulation in an aqueous environment. The geometric parameters of the systems were computed from their trajectories, including root mean square deviation (RMSD), root mean square fluctuation (RMSF), the radius of gyration (Rg), solvent accessible surface area (SASA), and the number of hydrogen bonds (NHBs) (Table 4). The RMSD is a typical way of determining the structural distance between coordinates which allows us to calculate the average distance between atoms in a group (e.g. backbone atoms of a protein). The average RMSD of the backbone atoms of free omicron spike protein, Omicron spike_Abemaciclib, Omicron spike_Dasatinib and Omicron spike_Spiperone complex were 0.278901594 ± 0.031966157 nm, 0.328851582 ± 0.025975243 nm, 0.308323815 ± 0.035772956 nm and 0.39048016 ± 0.042679318 nm respectively (Fig. 3**A**). This indicates that the compounds bind to the omicron spike protein, causing larger amplitudes of fluctuations. The average RMSD of the heavy atoms of the compounds-Abemaciclib, Dasatinib and Spiperone were found to be 0.396129844 ± 0.067303045 nm, 0.2 95270837 ± 0.09276118 nm and 0.752636825 ± 0.203613952 nm respectively (Fig. 3**B**) which suggests that the compounds did not undergo large conformational changes due to their stability within the active pocket of the omicron spike protein. RMSF is a measurement of a particle's average variation from a reference position over time. The RMSF plot shows stable fluctuations in free omicron spike protein and its complexes except for positions 483–486 and 527 in Omicron spike_Spiperone complex and residue 519 in Omicron spike_Dasatinib complex which experience fluctuations above 0.5 nm (Fig. 4). The gyration radius, which is a measure of structural compactness, was determined to be 1.791489131 ± 0.01812 1192 nm, 1.79507034 ± 0.02000475 nm, 1.834778621 ± 0.01906 795 nm, and 1.792068042 ± 0.015354762 nm, respectively (Fig. 5). The results indicate that the compound binding causes a decrease in the structural compactness of the spike protein. The total solvent accessible surface area (the surface area of a protein that interacts with its solvent molecules) for free omicron spike protein, Omicron spike_Abemaciclib, Omicron spike_Dasatinib and Omicron spike_Spiperone complex was found to be 96.21862 537 ± 3.188253865 nm^2, 100.6188232 ± 3.602129296 nm^2, 99.58 443457 ± 3.369326989 nm^2 and 98.73928472 ± 5.23296547 nm^2 respectively (Fig. 6). The increase in the total SASA upon interaction with the compounds indicate that the spike protein became less folded which enabled it to have more contact with the surrounding solvent molecules. The dynamics of the hydrogen bond network is crucial for understanding the protein stability in a solution. The intramolecular hydrogen bonds were found to be 124.8 761239 ± 6.974570909, 116.2367632 ± 6.214087794, 121.287712 3 ± 6.952060044 and 120.4625375 ± 7.516837444 (Fig. 7**A**). The results imply that the intramolecular hydrogen bonds within the omicron spike protein are decreased upon binding of the compounds. The intermolecular hydrogen bonds between the spike receptor and lead molecules were found to be 0.225774226 ± 0.4 50527496, 1.756243756 ± 1.04619476 and 1.623376623 ± 0.952 372294 for Omicron spike_Abemaciclib, Omicron spike_Dasatinib and Omicron spike_Spiperone complex respectively (Fig. 7**B**) and these intermolecular hydrogen bonds help to contribute towards the stabilization of the complexes between the omicron spike protein and compounds.

The highly coordinated modes of fluctuations for Omicron spike and Omicron spike complexed with the top 3 ranked compounds were studied using essential dynamics (ED). A covariance matrix was generated for this by selecting the protein's Cα atoms (N = 195). After diagonalizing the covariance matrix for free omicron spike protein, Omicron spike_Abemaciclib, Omicron spike_Dasatinib and Omicron spike_Spiperone, the trace of the covariance matrix was found to be 5.98045 nm^2, 5.0047 nm^2,

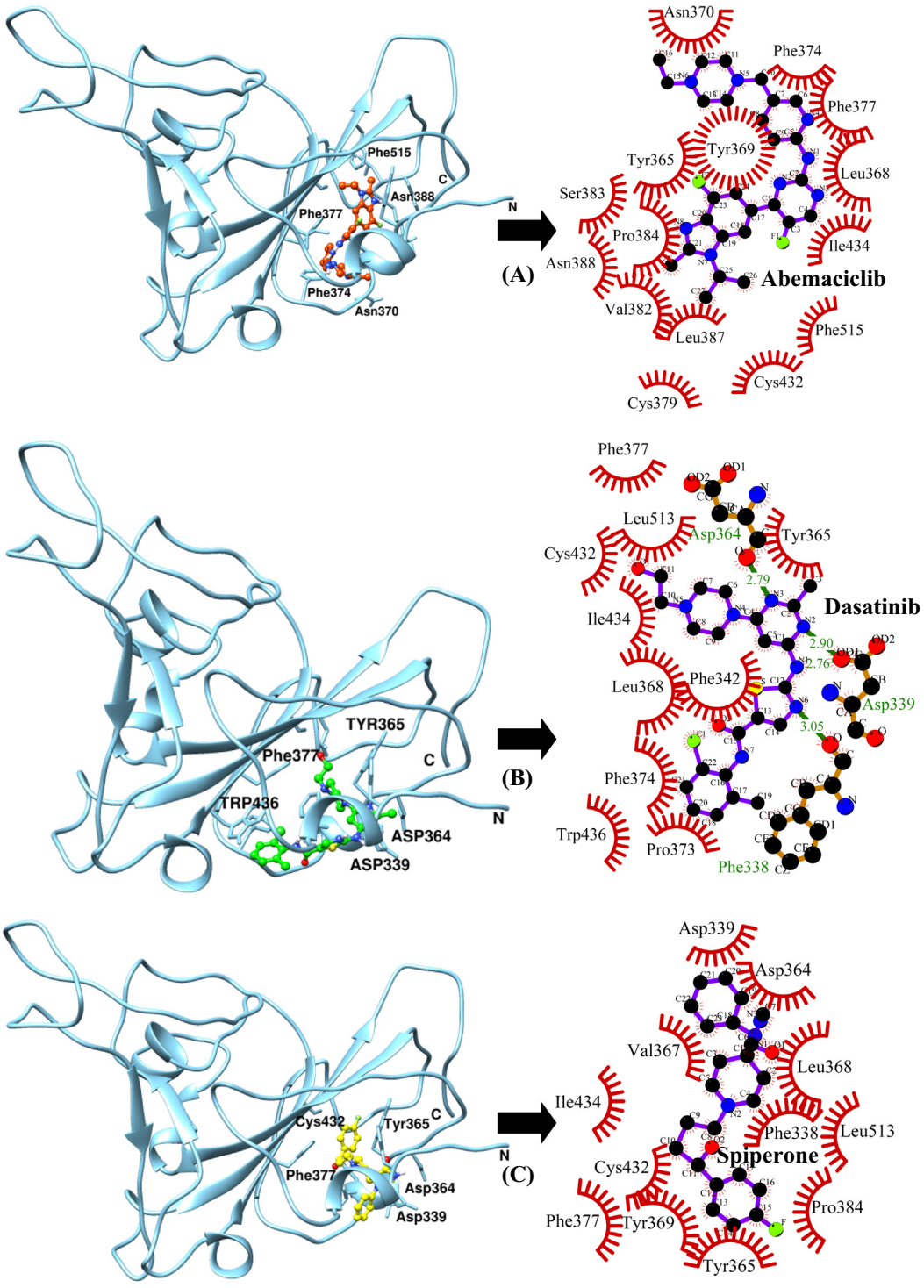

Fig. 2. Left panel shows the binding poses of the top 3 lead molecules within the active pocket of Omicron spike protein (**A)** Abemaciclib **(B)** Dasatinib and (**C)** Spiperone where the spike protein is represented in grey ribbon and the lead molecules in a ball and stick representation. The right-hand panel shows the molecular interactions between lead molecules and spike protein. Here, the hydrogen bonds are shown in a green dashed line and hydrophobic interactions with red semi-arcs.

6.31747 nm^2 and 7.47092 nm^2 respectively. The first few eigenvectors, out of a total of 585 (3 N), play a significant role in the system's fluctuations. The eigenvalue curve of Omicron spike_Dasatinib and Omicron spike_Spiperone complex were steeper than that of free omicron spike protein except for Omicron spike_Abemaciclib indicating that fewer eigenvectors are required to comprehend the same degree of total mean square fluctuations (Fig. 8). The Eigenvector 1 (PC1) contribution towards fluctuations in free omicron spike protein and Omicron spike_Abemaciclib, Omicron spike_Dasatinib and Omicron spike_Spiperone was determined to be 1.74856 nm^2 (29.2379%), 1.39182 nm^2 (27.8103%), 2.592 nm^2 (41.0291%) and 2.07159 nm^2 (27.7287%), respectively, with corresponding cosine values of 0.683886, 0.845428, 0.794308 and 0.868173. In free omicron spike protein, Omicron spike_Abemaciclib, Omicron spike_Dasatinib and Omicron spike_Spiperone, respectively, eigenvector 2 (PC2) contribution to

Table 3
Physicochemical characteristics of selected compounds.

Molecule Name	MW[a]	LogP[b]	HBA[c]	HBD[d]	TPSA[e](A^2)	RB[f]	Druglikeness
Salvianolic acid C	492.435	3.3063	10	6	177.89	8	−3.5203
Arbidol	477.422	4.1689	5	1	80	8	−1.164
Cepharanthine	606.717	6.7524	8	0	61.86	2	4.58
Abemaciclib	506.603	4.1154	8	1	75	7	6.2983
Osimertinib	499.617	3.4175	9	2	87.55	10	−5.4185
Trimipramine	294.44	4.1092	2	0	6.48	4	4.0901
Colforsin	410.505	1.3206	7	3	113.29	3	−4.6773
Ingenol	348.437	0.9134	5	4	97.99	1	−0.49807
Clofazimine	473.406	6.2781	4	1	39.99	4	1.9723
Tafenoquine	463.498	4.7717	6	2	78.63	10	−5.9887
Baicalin	446.363	−0.0032	11	6	183.21	4	0.34679
Baicalein	270.239	2.3357	5	3	86.99	1	0.28194
Cinanserin	340.49	3.8584	3	1	57.64	8	2.934
GC373	405.493	1.2677	8	4	116.76	11	−13.113
Boceprevir	519.684	1.3825	10	4	150.7	10	−8.7582
Bepridil	366.547	4.4044	3	0	15.71	10	1.468
Nelfinavir mesylate	567.792	4.4556	7	4	127.2	10	0.6687
Z-FA-FMK	386.422	2.1022	6	2	84.5	10	−11.445
Suramin	1297.29	−2.9082	29	12	534.03	16	−1.2647
Lopinavir	628.811	4.847	9	4	120	15	6.5929
Ritonavir	720.957	4.7152	11	4	202.26	18	−7.147
Dipyridamole	504.634	0.7916	12	4	145.44	12	0.43417
Dasatinib	488.014	3.6259	9	3	134.75	7	8.0376
Dronedarone	556.765	6.7266	7	1	97.23	17	0.70822
Remdesivir	602.583	0.3048	14	4	213.36	13	−21.381
Favipiravir	157.104	−1.7969	5	2	84.55	1	2.9436
Dolutegravir	419.383	0.1208	8	2	99.18	3	5.5879
β-D-N4-Hydroxycytidine (EIDD-1931)	259.217	−3.1512	9	5	134.85	2	−1.8924
Tipranavir	602.672	5.9823	7	2	113.97	11	−6.9229
Saquinavir	670.852	2.836	11	5	166.75	13	1.1609
Atazanavir	704.866	3.3709	13	5	171.22	18	−16.542
Azithromycin	748.992	1.6569	14	5	180.08	7	13.854
Spiperone	395.476	3.0219	5	1	52.65	6	9.9352
Alprostadil	354.485	4.045	5	3	94.83	13	−16.472
Ivermectin	875.102	4.7534	14	3	170.06	8	4.7349
Penciclovir	253.261	−1.6358	8	4	125.76	5	−2.6783

a: molecular weight b: partition coefficient between *n*-octanol and water c: number of hydrogen bond acceptors d: number of hydrogen bond donors e: topological polar surface area f: rotatable bond count.

Table 4
Average geometric properties of the systems with standard deviations in parentheses.

Systems	RMSD[a] (nm)		Rg[b] (nm)	Total SASA[c] (nm^2)	NHBS[d]	
	Protein	Ligand			Intramolecular	Intermolecular
Free Omicron spike protein	0.278901594 (0.031966157)	–	1.791489131 (0.018121192)	96.21862537 (3.188253865)	124.8761239 (6.974570909)	–
Omicron spike_Abemaciclib	0.328851582 (0.025975243)	0.396129844 (0.067303045)	1.79507034 (0.02000475)	100.6188232 (3.602129296)	116.2367632 (6.214087794)	0.225774226 (0.450527496)
Omicron spike_Dasatinib	0.308323815 (0.035772956)	0.295270837 (0.09276118)	1.834778621 (0.01906795)	99.58443457 (3.369326989)	121.2877123 (6.952060044)	1.756243756 (1.04619476)
Omicron spike_Spiperone	0.39048016 (0.042679318)	0.752636825 (0.203613952)	1.792068042 (0.015354762)	98.73928472 (5.232964547)	120.4625375 (7.516837444)	1.623376623 (0.952372294)

fluctuations was determined to be 0.851629 nm^2 (14.2402%), 0.799175 nm^2 (15.9684%), 0.614664 nm^2 (9.7296%) and 1.35787 nm^2 (18.1754%), with corresponding cosine values of 0.00296267, 0.0241793, 0.0791846 and 0.00316657. We chose only eigenvectors 1 and 2 for our investigations since they contribute more to total mean square fluctuations and their cosine values are less than 1 (sufficient conformational sampling). The free omicron spike protein is more compact and clustered than omicron spike-ligand complexes, indicating that its fluctuations are less coordinated (Fig. 9). The fluctuation represented by PC1 and PC2 is also projected as a free energy landscape. The Gibbs free energies of conformation sub-spaces of in free omicron spike protein, Omicron spike_Abemaciclib, Omicron spike_Dasatinib and Omicron spike_Spiperone were determined to be 0 to 7.87 kJ/mol, 0 to 8.88 kJ/mol, 0 to 8.17 kJ/mol and 0 to 8.3 kJ/mol, respectively (Fig. 10), showing that free omicron spike protein has more energetically favourable conformational transitions than its complexes. In addition, across the free energy landscape, a few meta-stable states or energy minima (in blue) were found in a free omicron spike protein and omicron spike-ligand complexes. Furthermore, at T = 300 K, the absolute entropy computed using the quasi-harmonic approximation method (Andricioaei and Karplus, 2001) was found to be 41977.5 J/molK, 42356.0 J/molK, 42269.8 J/molK and 41989.3 J/molK for free omicron spike protein, Omicron spike_Abemaciclib, Omicron spike_Dasatinib and Omicron spike_Spiperone respectively. The results indicate that the disorder or randomness in the omicron spike protein structure increases upon interaction with the lead molecules.

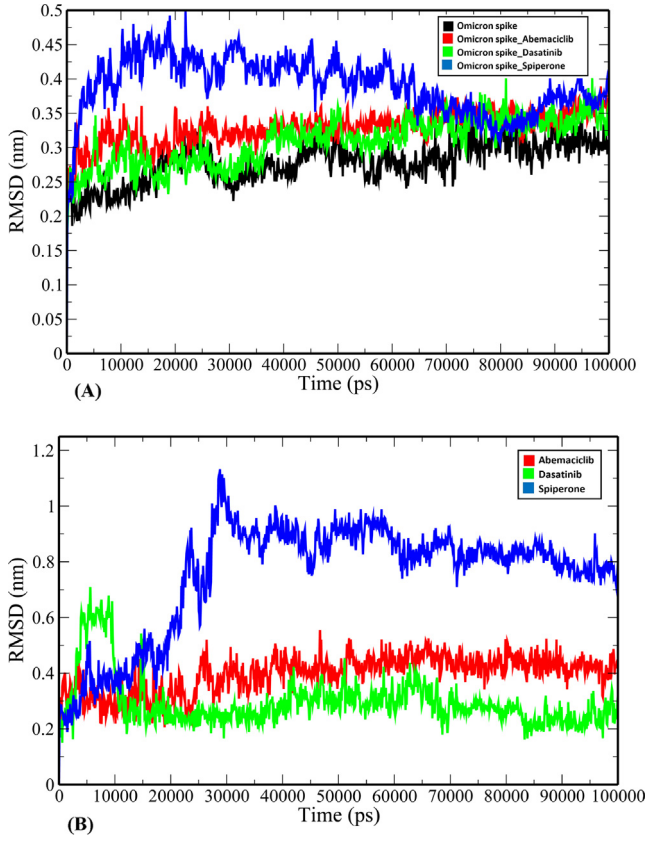

Fig. 3. RMSD (backbone atoms) of **(A)** free omicron spike protein and omicron spike-ligand complexes **(B)** compounds along 100 ns trajectories.

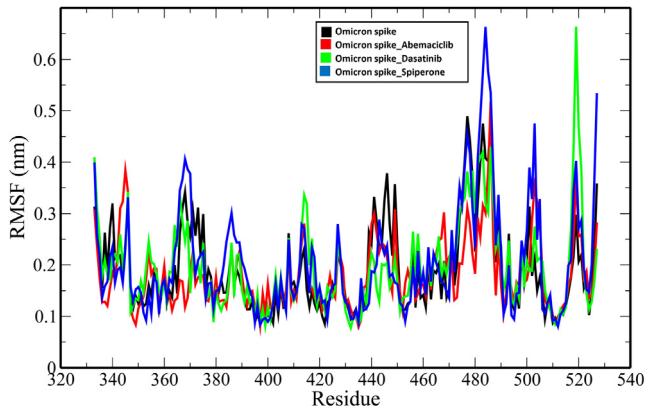

Fig. 4. RMSF plot showing atomic fluctuations of free omicron spike protein and omicron spike-ligand complexes.

4. Discussion

The increased number of new cases due to the new variant of concerns, SARS-CoV-2 omicron, offers a challenge to global health systems as the world fights COVID-19. With a significant number of mutations and deletions, the fifth variant of concern is thought to be more infectious than previously found variants (Gao et al., 2021). More clinical evidence is needed to determine the virus's actual pathogenicity, transmissibility, and ability to neutralize serum antibodies. Because there are no viable treatments for the previous variants as well, discovering therapeutic compounds for the omicron is a difficult challenge that will necessitate much scientific research. SARS-CoV-2 uses the spike glycoprotein to attach to the cellular receptor ACE2 to enter into the host cells and mediate its infectious cycle. Our current study is aimed at the identification of small molecules which can inhibit the interaction between omicron spike protein and ACE2. Using a set of 36 known antivirals for previous variants of SARS-CoV-2 and the recently solved experimental structure of omicron spike protein in complex with ACE2 (Han et al., 2022), we were able to evaluate whether these molecules could bind to the omicron spike protein. The protein–protein complex is stabilised by one salt bridge, ten hydrogen bonds, and 87 non-bonded interactions, according to PDBsum analysis. Abemaciclib, Dasatinib and Spiperone demonstrated a strong affinity for the omicron spike protein in molecular docking studies and their physicochemical property analysis revealed good drug-likeness scores. Abemaciclib is a cyclin-dependent kinase 4/6 (CDK4/6) inhibitor that is currently being used in combination with an aromatase inhibitor or fulvestrant to treat endocrine sensitive and resistant metastatic luminal breast cancer, respectively (El Hachem et al., 2021). Dasatinib (Sprycel; Bristol-Myers Squibb) is a tyrosine kinase inhibitor that was approved by the US Food and Drug Administration (FDA) in June 2006 for the treatment of adults with chronic myeloid leukaemia and Philadelphia-chromosome-positive acute lymphoblastic leukaemia who had developed resistance or intolerance to previous therapy (Kantarjian et al., 2006). Spiperone is an antagonist for the dopamine D2 receptor. It is not used even though it has antipsychotic properties. It's more commonly utilised as a pharmacological tool for studying neurotransmitter receptors (Davis, 2007). The molecular dynamics sim-

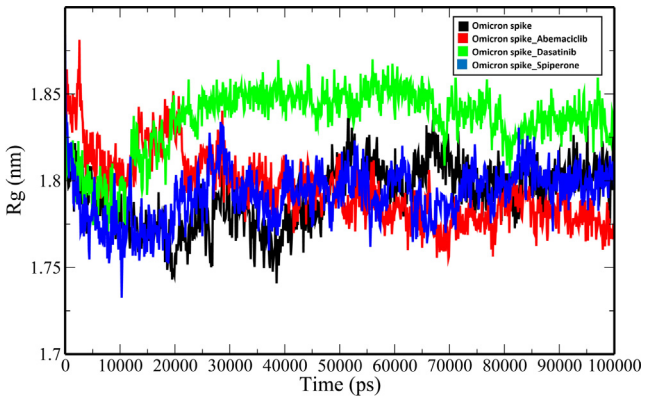

Fig. 5. Time-evolution of Rg trajectories of free omicron spike protein and omicron spike-ligand complexes.

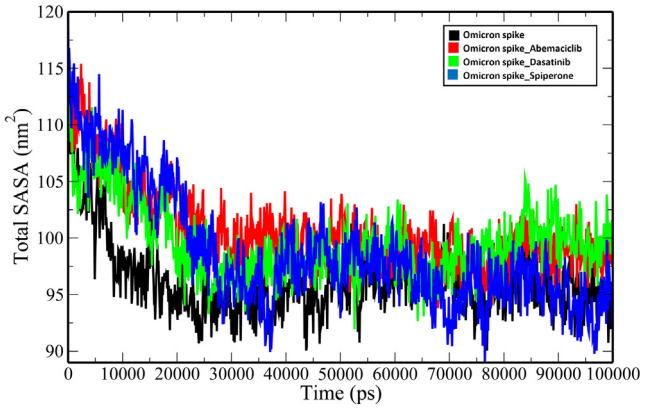

Fig. 6. Plot of total SASA of free omicron spike protein and omicron spike-ligand complexes.

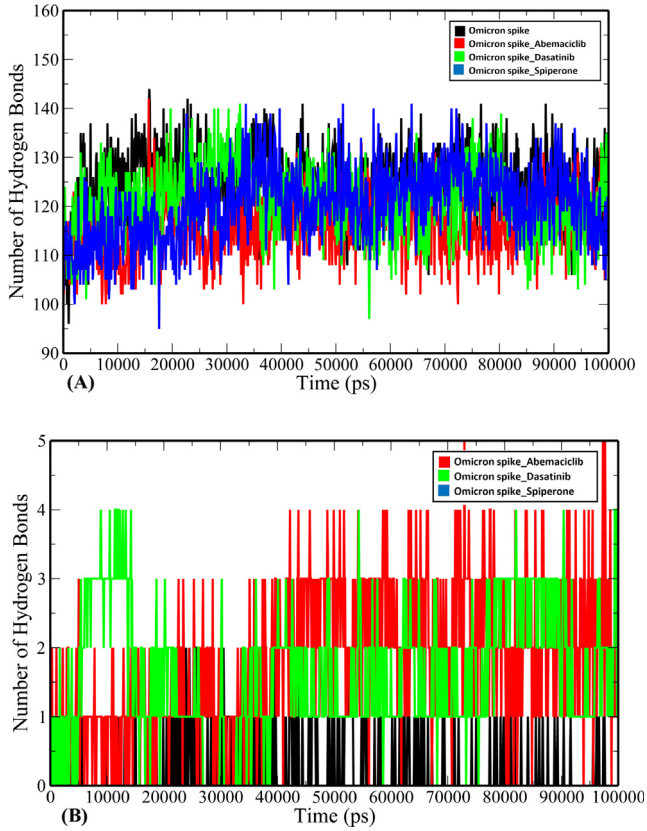

Fig. 7. Hydrogen bond analysis of free omicron spike protein and omicron spike-ligand complexes **(A)** intramolecular protein hydrogens **(B)** intermolecular protein–ligand hydrogen bonds.

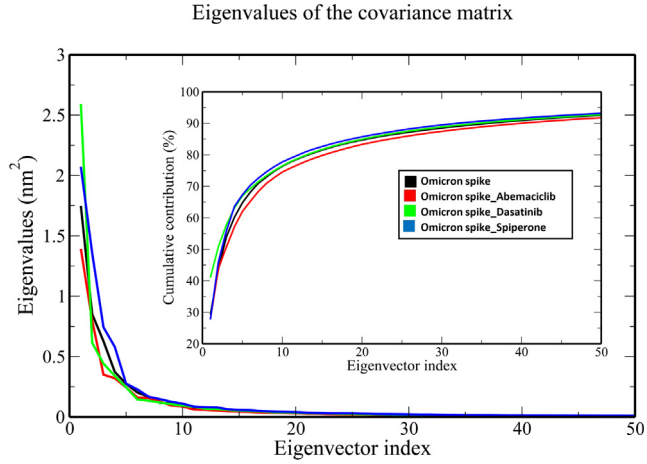

Fig. 8. Eigenvalue vs eigenvector index plot of free omicron spike protein and omicron spike-ligand complexes with the inset depicting cumulative contribution to overall fluctuation versus eigenvector index. The figure only shows the first fifty eigenvectors out of 585 eigenvectors (3 N where N = 195).

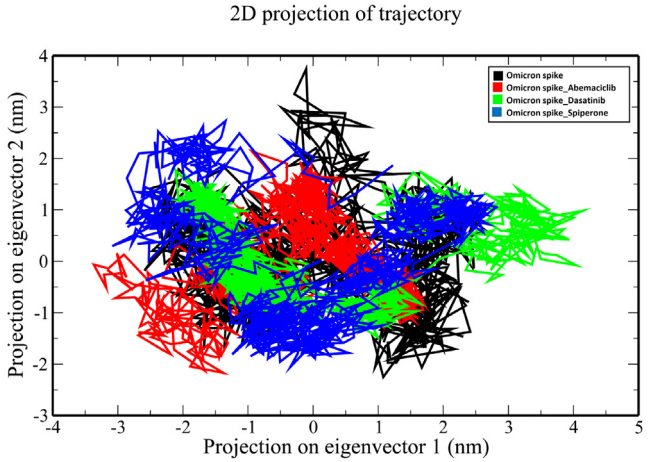

Fig. 9. Plot of two-dimensional projections of PC1 and PC2 for free omicron spike protein and omicron spike-ligand complexes.

ulation results revealed stability of the trajectories through 100 ns and displayed differences in the geometric properties between the free omicron protein and its complexes with the lead molecules. Essential dynamics and entropic analysis also indicate the modulation of the structure of the spike protein by these lead molecules indicating that these compounds can impair the function of the omicron spike protein. To determine the binding strength and thermodynamic parameters of interaction between omicron spike protein and the lead compounds, experimental approaches such as surface plasmon resonance (SPR) and isothermal titration calorimetry (ITC) as well as spectroscopic techniques are recommended. Despite the fact that the current research is totally computational, the outcomes of our studies will aid in further experimental investigations and the development of therapies for SARS-CoV-2 omicron infections.

5. Conclusion

The extremely contagious nature of the novel omicron variant necessitates the development of effective drug molecules to combat its worldwide spread. We found three candidate drugs Abemaciclib, Dasatinib and Spiperone with high binding affinity for omicron spike glycoprotein and good drug-likeness scores using molecular docking and physicochemical property analysis. The binding of the lead compounds causes aberrations in the structural properties of the omicron spike protein as revealed from molecular dynamics simulation investigations. These compounds could be developed into SARS-CoV-2 omicron entry inhibitors, which would help to reduce infection and spread.

Declaration of Competing Interest

The authors declare that they have no known competing financial interests or personal relationships that could have appeared to influence the work reported in this paper.

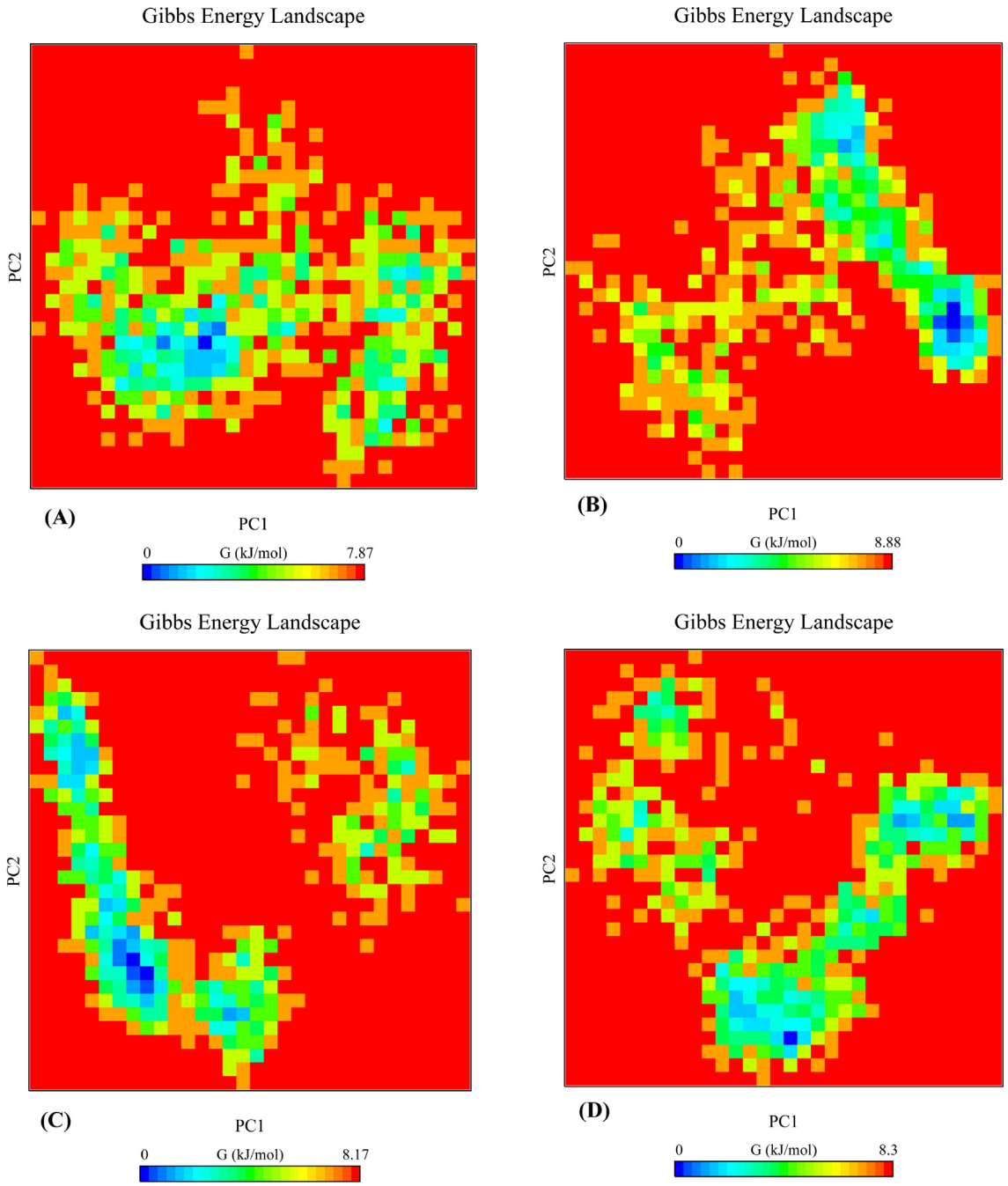

Fig. 10. Plot of Gibbs free energy landscapes of PC1 and PC2 for **(A)** free omicron spike **(B)** Omicron spike_Abemaciclib **(C)** Omicron spike_Dasatinib and **(D)** Omicron spike_Spiperone. The colour scale runs from blue to red, representing the lowest and maximum Gibbs free energy, respectively.

Acknowledgements

The authors would like to extend their sincere appreciation to the Researchers Supporting Project number (RSP-2021/306), King Saud University, Riyadh, Saudi Arabia.

References

Amadei, A., Linssen, A.B.M., Berendsen, H.J.C., 1993. Essential dynamics of proteins. Proteins Struct. Funct. Bioinforma. 17 (4), 412–425. https://doi.org/10.1002/prot.340170408.

Andricioaei, I., Karplus, M., 2001. On the calculation of entropy from covariance matrices of the atomic fluctuations. J. Chem. Phys. 115 (14), 6289–6292. https://doi.org/10.1063/1.1401821.

Davis, C., 2007. Spiperone. In: Enna, S.J., Bylund, D.B. (Eds.), XPharm: The Comprehensive Pharmacology Reference. Elsevier, New York, pp. 1–3.

El Hachem, G., Gombos, A., Awada, A., 2021. Abemaciclib, a third CDK 4/6 inhibitor for the treatment of hormone receptor-positive, human epidermal growth factor receptor 2-negative advanced or metastatic breast cancer. Expert Rev. Anticancer Ther. 21 (1), 81–92.

Gao, S.-J., Guo, H., Luo, G., 2021. Omicron variant (B.1.1.529) of SARS-CoV-2, a global urgent public health alert! J. Med. Virol. 94 (4), 1255–1256.

GISAID. (2021). Tracking of Variants. https://www.gisaid.org/hcov19-variants/ Date accessed: November 30, 2021.

Greaney, A.J., Starr, T.N., Gilchuk, P., Zost, S.J., Binshtein, E., Loes, A.N., Hilton, S.K., Huddleston, J., Eguia, R., Crawford, K.H.D., Dingens, A.S., Nargi, R.S., Sutton, R.E., Suryadevara, N., Rothlauf, P.W., Liu, Z., Whelan, S.P.J., Carnahan, R.H., Crowe, J.E., Bloom, J.D., 2021. Complete mapping of mutations to the SARS-CoV-2 spike

receptor-binding domain that escape antibody recognition. Cell Host Microbe 29 (1), 44–57.e9.
Gurung, A.B., 2020. In silico structure modelling of SARS-CoV-2 Nsp13 helicase and Nsp14 and repurposing of FDA approved antiviral drugs as dual inhibitors. Gene Rep. 21, 100860. https://doi.org/10.1016/j.genrep.2020.100860.
Halgren, T.A., 1996. Merck molecular force field. I. Basis, form, scope, parameterization, and performance of MMFF94. J. Comput. Chem. 17, 490–519. https://doi.org/10.1002/(SICI)1096-987X(199604)17:5/6<490::AID-JCC1>3.0.CO;2-P.
Han, P., Li, L., Liu, S., Wang, Q., Zhang, D.i., Xu, Z., Han, P.u., Li, X., Peng, Q.i., Su, C., Huang, B., Li, D., Zhang, R., Tian, M., Fu, L., Gao, Y., Zhao, X., Liu, K., Qi, J., Gao, G.F., Wang, P., 2022. Receptor binding and complex structures of human ACE2 to spike RBD from omicron and delta SARS-CoV-2. Cell 185 (4), 630–640.e10.
Harvey, W.T., Carabelli, A.M., Jackson, B., Gupta, R.K., Thomson, E.C., Harrison, E.M., Ludden, C., Reeve, R., Rambaut, A., Peacock, S.J., Robertson, D.L., 2021. SARS-CoV-2 variants, spike mutations and immune escape. Nat. Rev. Microbiol. 19 (7), 409–424.
Hess, B., Kutzner, C., Van Der Spoel, D., Lindahl, E., 2008. GRGMACS 4: Algorithms for highly efficient, load-balanced, and scalable molecular simulation. J. Chem. Theory Comput. 4, 435–447. https://doi.org/10.1021/ct700301q.
Kantarjian, H., Jabbour, E., Grimley, J., Kirkpatrick, P., 2006. Dasatinib. Nat. Rev. Drug Discov. 5 (9), 717–718.
Karim, S.S.A., Karim, Q.A., 2021. Omicron SARS-CoV-2 variant: a new chapter in the COVID-19 pandemic. Lancet 398 (10317), 2126–2128.
Kim, S., Thiessen, P.A., Bolton, E.E., Chen, J., Fu, G., Gindulyte, A., Han, L., He, J., He, S., Shoemaker, B.A., Wang, J., Yu, B.o., Zhang, J., Bryant, S.H., 2016. PubChem Substance and Compound databases. Nucleic Acids Res 44 (D1), D1202–D1213. https://doi.org/10.1093/nar/gkv951.
Kirchdoerfer, R.N., Cottrell, C.A., Wang, N., Pallesen, J., Yassine, H.M., Turner, H.L., Corbett, K.S., Graham, B.S., McLellan, J.S., Ward, A.B., 2016. Pre-fusion structure of a human coronavirus spike protein. Nature 531 (7592), 118–121.
Laskowski, R.A., 2009. PDBsum new things. Nucleic Acids Res. 37 (Database), D355–D359. https://doi.org/10.1093/nar/gkn860.
Laskowski, R.A., Swindells, M.B., 2011. LigPlot+: multiple ligand-protein interaction diagrams for drug discovery. J. Chem. Inf. Model. 51 (10), 2778–2786. https://doi.org/10.1021/ci200227u.
Lipinski, C.A., 2004. Lead- and drug-like compounds: the rule-of-five revolution. Drug Discov. Today. Technol. 1 (4), 337–341. https://doi.org/10.1016/j.ddtec.2004.11.007.
Liu, X., Shi, D., Zhou, S., Liu, H., Liu, H., Yao, X., 2018. Molecular dynamics simulations and novel drug discovery. Expert Opin. Drug Discov. 13 (1), 23–37.
Madu, I.G., Roth, S.L., Belouzard, S., Whittaker, G.R., 2009. Characterization of a highly conserved domain within the severe acute respiratory syndrome coronavirus spike protein S2 domain with characteristics of a viral fusion peptide. J. Virol. 83 (15), 7411–7421.
McConkey, B.J., Sobolev, V., Edelman, M., 2002. The performance of current methods in ligand–protein docking. Curr. Sci., 845–856
Millet, J.K., Whittaker, G.R., 2015. Host cell proteases: critical determinants of coronavirus tropism and pathogenesis. Virus Res. 202, 120–134.
Morris, G.M., Huey, R., Lindstrom, W., Sanner, M.F., Belew, R.K., Goodsell, D.S., Olson, A.J., 2009. AutoDock4 and AutoDockTools4: Automated docking with selective receptor flexibility. J. Comput. Chem. 30 (16), 2785–2791. https://doi.org/10.1002/jcc.21256.
O'Boyle, N.M., Banck, M., James, C.A., Morley, C., Vandermeersch, T., Hutchison, G.R., 2011. Open Babel: An open chemical toolbox. J. Cheminform. 3, 33. https://doi.org/10.1186/1758-2946-3-33.
Ou-Yang, S.-S., Lu, J.-Y., Kong, X.-Q., Liang, Z.-J., Luo, C., Jiang, H., 2012. Computational drug discovery. Acta Pharmacol. Sin. 33 (9), 1131–1140.
Park, J.-E., Li, K., Barlan, A., Fehr, A.R., Perlman, S., McCray, P.B., Gallagher, T., 2016. Proteolytic processing of Middle East respiratory syndrome coronavirus spikes expands virus tropism. Proc. Natl. Acad. Sci. 113 (43), 12262–12267.
Rastelli, G., Rio, A.D., Degliesposti, G., Sgobba, M., 2010. Fast and accurate predictions of binding free energies using MM-PBSA and MM-GBSA. J. Comput. Chem., NA–NA https://doi.org/10.1002/(ISSN)1096-987X10.1002/jcc.21372.
Sander, T., Freyss, J., von Korff, M., Rufener, C., 2015. DataWarrior: an open-source program for chemistry aware data visualization and analysis. J. Chem. Inf. Model. 55 (2), 460–473. https://doi.org/10.1021/ci500588j.
Tortorici, M.A., Veesler, D., 2019. Structural insights into coronavirus entry. Adv. Virus Res. 105, 93–116.
Veber, D.F., Johnson, S.R., Cheng, H.-Y., Smith, B.R., Ward, K.W., Kopple, K.D., 2002. Molecular properties that influence the oral bioavailability of drug candidates. J. Med. Chem. 45 (12), 2615–2623.
Walls, A.C., Park, Y.-J., Tortorici, M.A., Wall, A., McGuire, A.T., Veesler, D., 2020. Structure, function, and antigenicity of the SARS-CoV-2 spike glycoprotein. Cell 181 (2), 281–292.e6.
Walls, A.C., Tortorici, M.A., Bosch, B.-J., Frenz, B., Rottier, P.J.M., DiMaio, F., Rey, F.A., Veesler, D., 2016. Cryo-electron microscopy structure of a coronavirus spike glycoprotein trimer. Nature 531 (7592), 114–117.
World Health Organization. Classification of Omicron (B.1.1.529): SARS-CoV-2 variant of concern. November 26, 2021. https://www.who.int/news/item/26-11-2021-classification-of-omicron-(b.1.1.529)-sars-cov-2-variant-of-concern.
Xiang, R., Yu, Z., Wang, Y., Wang, L., Huo, S., Li, Y., Liang, R., Hao, Q., Ying, T., Gao, Y., Yu, F., Jiang, S., 2021. Recent advances in developing small-molecule inhibitors against SARS-CoV-2. Acta Pharm. Acta Pharmaceutica Sinica B. https://doi.org/10.1016/j.apsb:2021.06.016.